Green-Solvent-Processed Molecular Solar Cells**

Xiaofen Chen, Xiaofeng Liu, Mark A. Burgers, Ye Huang, and Guillermo C. Bazan*

Abstract: High-efficiency bulk heterojunction (BHJ) organic solar cells with power conversion efficiencies of more than 5 % can be fabricated using the green solvent 2-MeTHF. The active layers comprise a blend of a molecular semiconductor donor with intermediate dimensions (X2) and the soluble fullerene derivative [6,6]-phenyl-C_{61}-butyricacidoctylester ($PC_{61}BC_8$). A switch of the processing solvent from chloroform to 2-MeTHF leads to no negative impacts on the morphology and charge-transport properties of optimally performing BHJ films. Examinations by absorption spectroscopy, atomic force microscopy, and grazing incidence wide-angle X-ray scattering reveal no significant modification of morphology. These results show that green solvents can be excellent alternatives for large-area printing of high-performance organic photovoltaics (OPVs) and thus open new opportunities for sustainable mass production of organic solar cells and other optoelectronic devices.

Significant strides are needed in order to develop new technologies that have as core objectives renewable energy and environmental protection, while concurrently allowing mass manufacturing using nontoxic and chemically sustainable resources.[1–3] Organic solar cells (OSCs) produced by solution processing are a relevant case in point.[4–7] A promising vision of fabricating the active layer is through roll-to-roll manufacturing, which can minimize cost and the energy of production, and result in flexible and light-weight modules with reduced installation costs.[8] However, although the power conversion efficiencies (PCEs) of OSCs have steadily increased through improvements in materials design,[9–14] mechanistic insight,[15–19] and device architectures,[20–22] the vast majority of high-performance devices with bulk heterojunction (BHJ) structures are deposited out of chlorinated and/or aromatic solvents, for example, chlorobenzene. Such solvents are well recognized to be contaminants in drinking water and exhibit various toxicity levels.[23–26] It is worth noting that regulations are being enacted, particularly in the European Union, that have as a long term goal of the elimination of harmful and unsustainable chemicals and materials.[3]

Environmentally benign solvents have yet to be used to fabricate the most efficient BHJ blends. Reports have appeared that describe the use of conjugated polymers with side groups that increase the solubility in typically more polar benign solvents, such as N-methyl-2-pyrrolidone[27] and alcohol.[28] However, the extent to which these side groups influence solid-state morphology, for example miscibility with fullerene derivatives, is not well understood. It seems reasonable to us that molecules with less extended structures would be attractive candidates to explore the casting of active BHJ from green solvents, given their greater solubility relative to their macromolecular counterparts.

Here, we report the use of 2-methyltetrahydrofuran (2-MeTHF) for the fabrication of BHJ solar cells with PCE of approximately 5 %. 2-MeTHF can be obtained from furfural, which is derived from agricultural by-products.[29,30] It fits within the class of solvents sought from renewable resources and the concept of capitalizing on waste to generate useful chemicals. Moreover, the toxicity of 2-MeTHF is lower than that of commonly used halogenated and aromatic solvents, such as chlorobenzene and chloroform ($CHCl_3$).[31] 2-MeTHF is often considered a green-solvent substitute in organic syntheses, including organocatalysis, and pharmaceutical chemistry.[32–34]
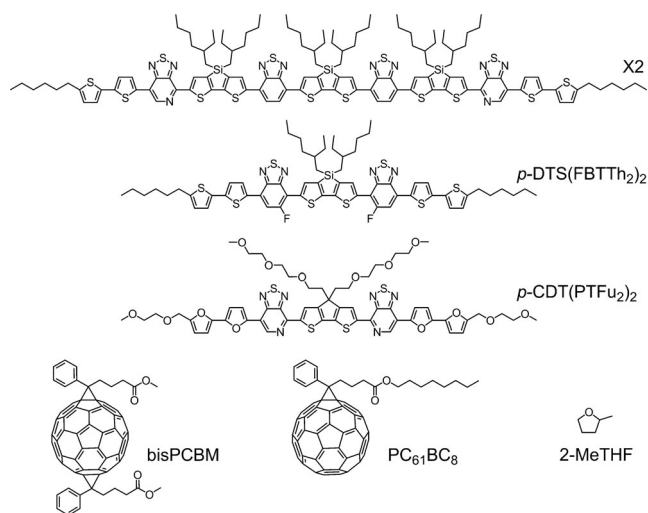
It seemed reasonable to examine X2 as the molecular donor (see Scheme 1 for molecular structures). This material exhibits high thermal stability and crystallinity together with good solubility in nonpolar solvents.[35] Moreover, PCEs of around 6.5 % have been achieved with blends of X2 with [6,6]-phenyl-C_{61}-butyric acid methyl ester ($PC_{61}BM$) from $CHCl_3$ in the absence of solvent additives. Second, the PCE values are maintained at similar levels across a range of D:A (wt:wt) compositions from 7:3 to 4:6; the BHJ performance is thus relatively resistant to compositional variations.[36] An initial set of tests demonstrated that the solubility of X2 in 2-MeTHF at room temperature is approximately 29 $mg\,mL^{-1}$, which proved to be sufficient for casting films of more than 300 nm thickness.

With respect to the fullerene acceptor, the solubility of widely used $PC_{61}BM$ in 2-MeTHF is less than 1 $mg\,mL^{-1}$, which is insufficient for spin coating. We thus examined doubly substituted bisPCBM and a derivative with a longer alkyl chain, $PC_{61}BC_8$, and determined solubilities higher than 15 $mg\,mL^{-1}$ and 9 $mg\,mL^{-1}$, respectively. Initial efforts to screen device performances with X2:bisPCBM demonstrated

[*] X. Chen, Dr. X. Liu, M. A. Burgers, Dr. Y. Huang,
Prof. Dr. G. C. Bazan
Center for Polymers and Organic Solids, Department of Chemistry
and Biochemistry, University of California, Santa Barbara
Santa Barbara, CA 93106 (USA)
E-mail: bazan@chem.ucsb.edu

Scheme 1. Molecular structures of X2, *p*-DTS(FBTTh$_2$)$_2$, *p*-CDT(PTFu$_2$)$_2$, bisPCBM, PC$_{61}$BC$_8$, and 2-MeTHF.

Figure 2. *J–V* plots of X2:PC$_{61}$BC$_8$ hole-only diodes (25 mg mL^{-1} total concentration, D:A = 50:50, wt/wt) prepared from CHCl$_3$ and 2-MeTHF.
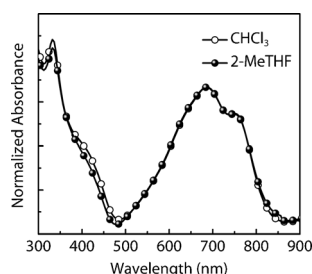

Figure 1. Thin-film UV-Vis absorption spectra of 50:50 X2:PC$_{61}$BC$_8$ blend obtained from 2-MeTHF and CHCl$_3$ from solutions containing 25 mg mL^{-1} total semiconductor content.

consistently poorer performance relative to X2:PC$_{61}$BC$_8$ (see the Supporting Information, Figure S1). Emphasis was therefore placed on examination of the X2:PC$_{61}$BC$_8$ blend.

The absorption spectra of X2:PC$_{61}$BC$_8$ blends cast from 2-MeTHF and CHCl$_3$ (Figure 1) exhibit nearly identical characteristics in the 300–900 nm range, which are also very similar to that observed with X2:PC$_{61}$BM films prepared from CHCl$_3$.[36] The surface roughness and film morphology, as determined by atomic force microscopy (AFM), are also not greatly affected by the choice of solvent (see Figure S2). These characterization tools thus do not show any obvious differences in possible changes in surface features or film quality that would be detrimental factors for device fabrication.

Hole-only diodes were fabricated to determine the effect of processing that the active layer from 2-MeTHF would have on hole transport. Current density–voltage characteristics (*J–V*) in the dark (see Figure S3) were collected and the Mott–Gurney law for the space-charge-limited current (SCLC) was used to determine the zero field mobility of the layer.[38] Analysis of the results shown in Figure 2 provided hole mobilities of 2.1×10^{-4} cm^2 V^{-1} s^{-1}(CHCl$_3$) and 5.6×10^{-4} cm^2 V^{-1} s^{-1} (2-MeTHF). Indeed, the film cast from 2-MeTHF exhibited slightly higher hole mobility, a desirable
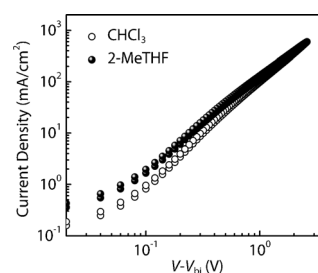
quality for extraction of photoinduced charge carriers in photovoltaic devices.[39]

BHJ devices fabricated from either CHCl$_3$ or 2-MeTHF were characterized in parallel to investigate the photovoltaic properties. The device structure adopted for our studies is ITO/MoO$_x$/X2:PC$_{61}$BC$_8$/Ca/Al. An examination of previous work[36] led us to focus on the fabrication of X2:PC$_{61}$BC$_8$ with 60:40 and 50:50 ratios. These two ratios provide devices with very similar characteristics (Table S4). Table 1 provides a summary of device characteristics for X2:PC$_{61}$BC$_8$ (50:50), the average values correspond to the examination of at least 20 devices. Figure 3 a provides the current density–voltage

Table 1: Photovoltaic properties of devices processed out of different solvents at different concentrations (X2:PC$_{61}$BC$_8$ = 50:50).

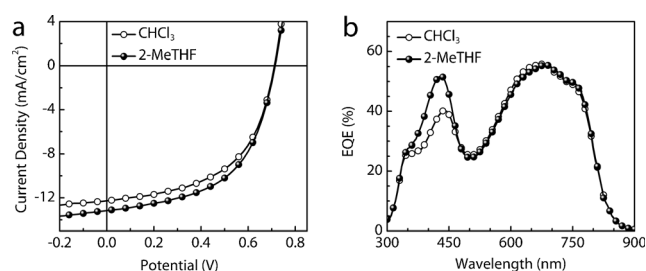| Solvent	Conc. [mg mL^{-1}]	J_{SC} [mA cm^{-2}]	V_{OC} [V]	FF [%]	PCE [%] Best	PCE [%] Avg.
CHCl$_3$	20	9.6 ± 0.3	0.72 ± 0.02	62 ± 1	4.5	4.3
	25	11.5 ± 0.3	0.72 ± 0.01	54 ± 2	4.7	4.6
	30	12.3 ± 0.2	0.71 ± 0.03	52 ± 2	4.7	4.6
2-MeTHF	20	10.3 ± 0.2	0.72 ± 0.02	59 ± 2	4.6	4.4
	25	12.3 ± 0.2	0.72 ± 0.02	55 ± 1	5.1	4.8
	30	12.5 ± 0.3	0.72 ± 0.02	53 ± 2	4.9	4.7

Figure 3. a) *J–V* characteristics, b) EQE curves of the optimal performance measured from films prepared from 2-MeTHF and CHCl$_3$.

characteristics (*J-V*) of the optimal device obtained from 2-MeTHF from which a PCE of 5.1% is demonstrated. Correspondingly, the best-performing device processed from CHCl$_3$ shows a PCE of 4.7%. Both devices show low leakage in the *J–V* plots in the dark (Figure S5). The external quantum efficiency (EQE) curves of the best performance devices are

provided in Figure 3b. As observed, devices show similar quantum efficiencies in the range from 500 to 800 nm, although for reasons not yet understood, the device with 2-MeTHF shows slightly higher quantum efficiencies near 450 nm.

Grazing incidence wide-angle X-ray scattering (GIWAXS) was used to investigate structural order in the blends.[40] Out-of-plane and in-plane reflection profiles are shown in Figure 4a,b. Films that were spin-cast from 2-
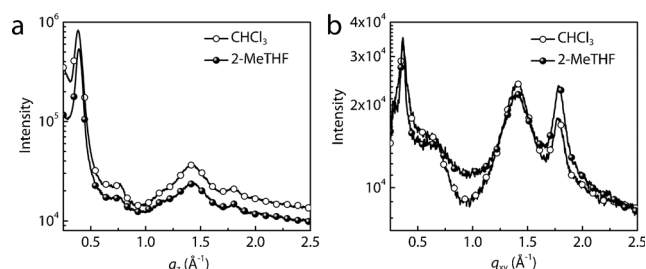

Figure 4. GIWAXS study of X2:PC$_{61}$BC$_8$ blend films (25 mg mL^{-1} total concentration, D:A = 50:50) prepared from CHCl$_3$ and 2-MeTHF: (a) and (b) are ± sector profiles along the nearly out-of-plane and in-plane directions, respectively.

MeTHF or CHCl$_3$ exhibit similar peaks: in-plane direction, π–π stacking at $q = 1.8$ Å^{-1} and alkyl-chain packing in the out-of-plane direction, at $q = 0.39$ Å^{-1}.[36] Crystallite correlation lengths (CCL) values determined using the (100) peak at $q = 0.39$ Å^{-1} were found to be 11.9 nm (CHCl$_3$) and 12.4 nm (2-MeTHF). A similar analysis for the (010) peak in-plane direction resulted in CCL values of 7.5 nm (CHCl$_3$) and 6 nm (2-MeTHF). These similarities suggest that crystallite features of X2 obtained from 2-MeTHF and CHCl$_3$ are similar, thereby demonstrating the similar ability of the two solvents to organize the BHJ components within the timescale of film formation.

It seemed appropriate to discuss two additional donor molecules in order to begin the identification of relevant desirable molecular and/or bulk features that enable processing with environmental solvent. One example involves the well-studied molecule p-DTS(FBTTh$_2$)$_2$, which has garnered significant attention and for which substantial device optimization protocols and morphological characterization exist.[41] For the purpose of our studies, p-DTS(FBTTh$_2$)$_2$ has no detectable solubility in 2-MeTHF and is thus not useful.

The second example involves p-CDT(PTFu$_2$)$_2$, which contains structural modifications for increasing the solubility in polar solvents. Specifically, alkyl side chains were exchanged for ethylene glycol side chains, and bithiophene moieties for bifuran building blocks.[42] However, p-CDT-(PTFu$_2$)$_2$:PC$_{61}$BC$_8$ devices fabricated from 2-MeTHF show no photovoltaic activity (see Figure S6). Examination by X-ray diffraction techniques shows no evidence of crystallization in the films (Figure S7). Thus, in the case of p-CDT(PTFu$_2$)$_2$, the molecular fragments that are included within the molecular structure to improve miscibility in polar solvents lead to resistance to crystallization in the bulk. Crystalline content is

a feature associated with high-performance molecular photovoltaic films.

In conclusion, we have shown that molecular solar cells with power conversion efficiencies over 5% can be fabricated by processing X2:PC$_{61}$BC$_8$ blends from 2-MeTHF. This solvent is derived from agricultural by-products and is considerably less toxic than widely used aromatic or halogenated alternatives. The donor component X2 was chosen on the basis that blends with PC$_{61}$BM can perform well across a wide composition range in the absence of an additive or thermal processing. It is worth noting that the X2:PC$_{61}$BC$_8$ blend provides slightly higher efficiencies from 2-MeTHF relative to the more conventional CHCl$_3$ as solvent. Although highly successful when processed from halogenated aromatic solvents, p-DTS(FBTTh$_2$)$_2$ is not suitable because of solubility limitations in polar solvents. In the case of p-CDT(PTFu$_2$)$_2$, the structural components included to aid in solubility lead to a resistance toward crystallization, a feature which we find important for attaining useful molecular BHJ morphologies. Altogether, these findings open new opportunities for considering mass production of organic solar cells, and other optoelectronic devices. It also highlights that substantial molecular design may not be fundamentally necessary for opening environmentally benign processing.

[1] J. H. Clark, V. Budarin, F. E. I. Deswarte, J. J. E. Hardy, F. M. Kerton, A. J. Hunt, R. Luque, D. J. Macquarrie, K. Milkowski, A. Rodriguez, O. Samuel, S. J. Tavener, R. J. White, A. Wilson, *Green Chem.* **2006**, *8*, 853–860.

[2] E. S. Beach, Z. Cui, P. T. Anastas, *Energy Environ. Sci.* **2009**, *2*, 1038–1049.

[3] J. Sherman, B. Chin, P. D. Huibers, R. Garcia-Valls, T. A. Hatton, *Environ. Health Perspect.* **1998**, *106*, 253–271.

[4] X. Guo, M. Zhang, C. Cui, J. Hou, Y. Li, *ACS Appl. Mater. Interfaces* **2014**, *6*, 8190–8198.

[5] K.-S. Chen, H.-L. Yip, C. W. Schlenker, D. S. Ginger, A. K.-Y. Jen, *Org. Electron.* **2012**, *13*, 2870–2878.

[6] D. J. Burke, D. J. Lipomi, *Energy Environ. Sci.* **2013**, *6*, 2053–2066.

[7] I. Burgués-Ceballos, F. Machui, J. Min, T. Ameri, M. M. Voigt, Y. N. Luponosov, S. A. Ponomarenko, P. D. Lacharmoise, M. Campoy-Quiles, C. J. Brabec, *Adv. Funct. Mater.* **2014**, *24*, 1449–1457.

[8] R. Søndergaard, M. Hösel, D. Angmo, T. T. Larsen-Olsen, F. C. Krebs, *Mater. Today* **2012**, *15*, 36–49.

[9] Y.-J. Cheng, S.-H. Yang, C.-S. Hsu, *Chem. Rev.* **2009**, *109*, 5868–5923.

[10] B. Carsten, F. He, H. J. Son, T. Xu, L. Yu, *Chem. Rev.* **2011**, *111*, 1493–1528.

[11] J. Chen, Y. Cao, *Acc. Chem. Res.* **2009**, *42*, 1709–1718.

[12] I. McCulloch, R. S. Ashraf, L. Biniek, H. Bronstein, C. Combe, J. E. Donaghey, D. I. James, C. B. Nielsen, B. C. Schroeder, W. Zhang, *Acc. Chem. Res.* **2012**, *45*, 714–722.

[13] N. Blouin, M. Leclerc, *Acc. Chem. Res.* **2008**, *41*, 1110–1119.

[14] Y. Li, *Acc. Chem. Res.* **2012**, *45*, 723–733.

[15] A. J. Moulé, K. Meerholz, *Adv. Mater.* **2008**, *20*, 240–745.

[16] J. Peet, J. Y. Kim, N. E. Coates, W. L. Ma, D. Moses, A. J. Heeger, G. C. Bazan, *Nat. Mater.* **2007**, *6*, 497–500.

[17] P. Zalar, M. Kuik, N. A. Ran, J. A. Love, T.-Q. Nguyen, *Adv. Energy Mater.* **2014**, DOI: 10.1002/anem.201400438.

[18] P. M. Beaujuge, J. M. J. Fréchet, *J. Am. Chem. Soc.* **2011**, *133*, 20009–20029.

[19] B. A. Collins, J. E. Cochran, H. Yan, E. Gann, C. Hub, R. Fink, C. Wang, T. Schuettfort, C. R. McNeill, M. L. Chabinyc, H. Ade, *Nat. Mater.* **2012**, *11*, 536–543.

[20] J. You, L. Dou, K. Yoshimura, T. Kato, K. Ohya, T. Moriarty, K. Emery, C.-C. Chen, J. Gao, G. Li, Y. Yang, *Nat. Commun.* **2013**, *4*, 1446.

[21] G. Yu, J. Gao, J. C. Hummelen, F. Wudl, A. J. Heeger, *Science* **1995**, *270*, 1789–1791.

[22] S. K. Hau, H.-L. Yip, A. K.-Y. Jen, *Polym. Rev.* **2010**, *50*, 474–510.

[23] D. Calamari, S. Galassi, F. Setti, M. Vighi, *Chemosphere* **1983**, *12*, 253–262.

[24] G. Van Hoogen, A. Opperhuizen, *Environ. Toxicol. Chem.* **1988**, *7*, 213–219.

[25] P. T. Heitmuller, T. A. Hollister, P. R. Parrish, *Bull. Environ. Contam. Toxicol.* **1981**, *27*, 596–604.

[26] http://www.epa.gov/ttn/atw/hlthef/chlorobe.html.

[27] Y. Chen, S. Zhang, J. Wu, J. Hou, *Adv. Mater.* **2014**, *26*, 2744–2749.

[28] C. Duan, W. Cai, B. B. Y. Hsu, C. Zhong, K. Zhang, C. Liu, Z. Hu, F. Huang, G. C. Bazan, A. J. Heeger, Y. Cao, *Energy Environ. Sci.* **2013**, *6*, 3022–3034.

[29] Y. Gu, F. Jérôme, *Chem. Soc. Rev.* **2013**, *42*, 9550–9570.

[30] J. H. Clark, L. A. Pfaltzgraff, V. L. Budarin, A. J. Hunt, M. Gronnow, A. S. Matharu, D. J. Macquarrie, J. R. Sherwood, *Pure Appl. Chem.* **2013**, *85*, 1625–1631.

[31] V. Antonucci, J. Coleman, J. B. Ferry, N. Johnson, M. Mathe, J. P. Scott, J. Xu, *Org. Process Res. Dev.* **2011**, *15*, 939–941.

[32] V. Pace, P. Hoyos, L. Castoldi, P. Domínguez de María, A. R. Alcántara, *ChemSusChem* **2012**, *5*, 1369–1379.

[33] S. Shanmuganathan, D. Natalia, A. van den Wittenboer, C. Kohlmann, L. Greiner, P. Domínguez de María, *Green Chem.* **2010**, *12*, 2240–2245.

[34] Y. Simeó, J. V. Sinisterra, A. R. Alcántara, *Green Chem.* **2009**, *11*, 855–862.

[35] X. Liu, Y. Sun, L. A. Perez, W. Wen, M. F. Toney, A. J. Heeger, G. C. Bazan, *J. Am. Chem. Soc.* **2012**, *134*, 20609–20612.

[36] Y. Huang, X. Liu, C. Wang, J. T. Rogers, G. M. Su, M. L. Chabinyc, E. J. Kramer, G. C. Bazan, *Adv. Energy Mater.* **2014**, DOI: 10.1002/anem.201301886.

[37] Y. Zhang, P. W. M. Blom, *Appl. Phys. Lett.* **2011**, *98*, 143504.

[38] A. Rose, *Phys. Rev.* **1955**, *97*, 1538–1544.

[39] M. M. Mandoc, L. J. A. Koster, P. W. M. Blom, *Appl. Phys. Lett.* **2007**, *90*, 133504.

[40] J. Rivnay, S. C. B. Mannsfeld, C. E. Miller, A. Salleo, M. F. Toney, *Chem. Rev.* **2012**, *112*, 5488–5519.

[41] T. S. Van der Poll, J. A. Love, T.-Q. Nguyen, G. C. Bazan, *Adv. Mater.* **2012**, *24*, 3646–3649.

[42] Z. B. Henson, P. Zalar, X. Chen, G. C. Welch, T.-Q. Nguyen, G. C. Bazan, *J. Mater. Chem. A* **2013**, *1*, 11117–11120.